SEGMENTATION OF FETAL ENVELOPE FROM 3D ULTRASOUND IMAGES BASED ON PIXEL INTENSITY STATISTICAL DISTRIBUTION AND SHAPE PRIORS

*Sonia Dahdouh**   *Antoine Serrurier**   *Gilles Grangé†*   *Elsa D. Angelini**   *Isabelle Bloch**

* Institut Mines-Telecom, Telecom ParisTech, LTCI CNRS, Paris, France
† Maternité Port Royal AP-HP, Groupe Hospitalier Cochin Saint Vincent De Paul, Paris, France.

ABSTRACT

This paper presents a novel shape-guided variational segmentation method for extracting the fetus envelope on 3D obstetric ultrasound images. Indeed, due to the inherent low quality of these images, classical segmentation methods tend to fail at segmenting these data. To compensate for the lack of contrast and of explicit boundaries, we introduce a segmentation framework that combines three different types of information: pixel intensity distribution, shape prior on the fetal envelope and a back model varying with fetus age. The intensity distributions, different for each tissue, and the shape prior, encoded with Legendre moments, are added as energy terms in the functional to be optimized. The back model is used in a post-processing step. Results on 3D ultrasound data are presented and compared to a set of manual segmentations. Both visual and quantitative comparisons show the satisfactory results obtained by this method on the tested data.

Index Terms— 3D Ultrasound, level-set, Legendre shape-prior, statistical prior, fetus back model, obstetric imaging

1. INTRODUCTION

Ultrasound (US) is the main imaging modality being used during pregnancy follow up to assess fetal development. Being low cost and non invasive, it is routinely used to measure classical biometry development markers such as the fetus volume, the bi-parietal diameter or the crown-rump length. However, due to the inherent poor visual quality of US data, automatic or semi-automatic computation of such criteria remains an issue. Indeed, speckle noise, low contrast, lack of explicit boundaries, occlusions caused by surrounding tissues or attenuation are examples of artifacts making such data so difficult to exploit automatically and explain why standard segmentation methods fail on these images.

Many papers have addressed the problem of segmentation on US data, however only few of them dealt specifically with the problem of the segmentation of the fetus envelope on 3D US data [1]. In [2], Conditional Random Fields were used in combination with wavelet-based textural features and Support Vector Machine classifier to segment 2D fetal ultrasound images. Image partitioning into fetus and background pixels was learned from their relative positions on a training set. Such an approach assumes that the fetus has the same position and orientation in all the images, which is not realistic when dealing with 3D ultrasound data as illustrated in Figure 1.

In [3], adaptive statistical distributions of gray-level intensities were used within a level-set framework to separate amniotic fluid,

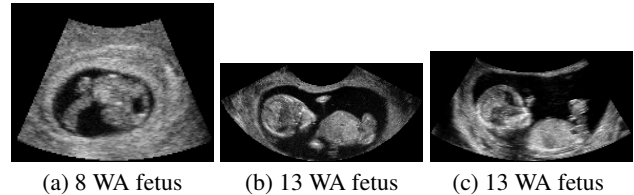(a) 8 WA fetus   (b) 13 WA fetus   (c) 13 WA fetus

Fig. 1. Slices of three 3D US data at different stages of gestation (WA: weeks of amenorrhea)

modeled with an exponential distribution, from maternal and fetal tissues, modeled with a Rayleigh distribution on 3D ultrasound data. The authors also extended their work to additional types of distributions allowing them to handle different types of fetal ultrasound images. While the method was useful for separating the amniotic fluid from the union of the fetus and the uterus, the separation of the fetus from the uterus was not straightforward.

In this paper, we propose to integrate a shape constraint into a 3D multi-phase variational segmentation approach, extending the two-phase framework introduced in [3] and taking advantage of a shape prior encoded with Legendre moments as done in [4], [5] and [6]. Variability of the fetus shape and position is handled via a set of learned shape models, as an original feature of the proposed approach. Finally, we propose a new post-processing step exploiting a set of back models to separate the fetus from other connected structures. Results on 3D fetal ultrasound images are presented in the Section 4.

2. INTRODUCING GRAY-LEVEL STATISTICAL DISTRIBUTIONS INTO A MULTI-PHASE LEVEL-SET FRAMEWORK

With the aim of separating maternal tissues from fetal ones while keeping apart the maternal ones from the amniotic fluid, the idea of using more than two phases with homogeneity priors has emerged and led us to extend the work presented in [3] to a multi-phase framework. Following [7], we express the minimal partitioning segmentation problem for multiple objects as follows:

Let Ω be a bounded and open subset of $\mathbf{R}^3$ and $I : \Omega \rightarrow \mathbf{R}$ an image. A given set of closed curves $\{C_1, C_2, ...C_n\}$ defines a partition of the image domain in a set of 2^n phases. In the case of two level-set functions, embedding these curves as the zero-level of signed functions $\{\phi_j\}$, the image segmentation into four phases is performed using the following energy [7]:

$$E_{im} = \sum_{i=1}^{4} \int_{\Omega} |I(x) - c_i|^2 \chi_i(x)\mathrm{d}x + \sum_{j=1}^{2} \nu \int_{\Omega} |\nabla H(\phi_j)|\mathrm{d}x \quad (1)$$

where $\nu \geq 0$ is a fixed parameter (set to 0.5 in our experiments), χ_i is the characteristic function associated with each phase, c_i is the average intensity inside each phase and H is the Heaviside function computed on each level-set ϕ_j, ϕ_j being positive inside each curve and negative outside.

While in the original Vese and Chan formulation [7] the homogeneity measure is the mean value of the considered region, the segmentation method here relies on *a priori* knowledge of the statistical distribution of gray-levels inside each region [3]. The intensities of the pixels belonging to the fetal and maternal tissues were modeled using respectively a Rayleigh and a Gamma distribution while the amniotic fluid was modeled using an Exponential one. As shown in [3], the Gamma and the Rayleigh distributions were able to capture the statistics of the maternal or fetal regions. Results of the segmentation procedure using this multi-phase framework are illustrated in Figure 2 (c). The use of two different statistical distributions enables to capture small differences that could separate maternal from fetal tissues but is not sufficient to achieve a perfect separation as shown in Figure 2 (c). This task requires an additional information based on a shape prior on the fetal body envelope, as described next.
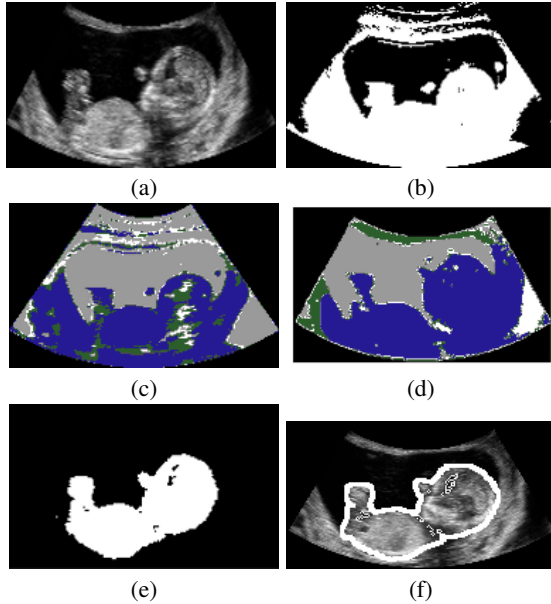

Fig. 2. Segmentation of a fetus at 12 WA. (a) Original slice of a 3D volume. (b) Segmentation with the two-phase framework from [3], (c) with the four-phase framework with no shape constraint (gray, white, blue and green corresponding to the 4 phases), (d) with the four-phase one with shape constraint, and (e) with post-processing for the fetus envelope. (f) Segmented fetus envelope overlaid on the US image.

3. SHAPE CONSTRAINT

Numerous methods have been proposed to constrain shape in a level-set based segmentation energy functional. In [8], a PCA analysis is performed on the level-set functions of a training set of shapes. In [9] the optimization is done on the first few eigenmodes. A non linear statistical shape model was introduced by Cremers *et al.* [10] while an implicit shape prior based on an active shape model was introduced by Rousson *et al.* [11]. More recently, Foulonneau *et al.* [4] proposed a geometric shape prior computed through the distance between the Legendre moments of a set of representative shapes and

the currently segmented one. In [6] a statistical shape model was built from the Legendre moments of a set of training shapes in a PCA reduced feature space while in [5] the shape prior built from Legendre moments was integrated into a fuzzy region competition framework for cardiac segmentation on CT-images. Since fetus positions and morphologies vary greatly, the use of a unique shape prior seems difficult. Thus, as in [4], we propose to handle this variability by using multiple shape priors. Inspired by the two previous methods, the one proposed in this paper optimizes, within a multiphase level-sets framework, a prior model represented by the distance computed between the currently determined shape, represented by its Legendre moments and a set of Legendre moments computed on a training set as explained next.

3.1. Shape encoding with Legendre moments

Let $I : [-1, 1]^3 \to \mathbf{R}$ be a 3D binary image encoding a shape where spatial coordinates are normalized in $[-1, 1]$. The $(p + q + r)^{th}$ order 3D Legendre moments of the image are defined as:

$$L_{pqr} = \lambda_{pqr} \int_{[-1,1]^3} P_p(x)P_q(y)P_r(z)I(x,y,z)\mathrm{d}x\mathrm{d}y\mathrm{d}z \quad (2)$$

with $\lambda_{pqr} = \frac{(2p+1)(2q+1)(2r+1)}{8}$, $(p,q,r) \in \mathbf{N}^+$ and P_i ($i = p, q, r$), the Legendre polynomial defined as:

$$P_i(x) = \sum_{k=0, i-k=even}^{i} (-1)^{\frac{i-k}{2}} \frac{1}{2^i} \frac{(i+k)!x^k}{(\frac{i-k}{2})!(\frac{i+k}{2})!k!} \quad (3)$$

Working with a finite number N of moments (set to 60 in all our experiments) for each dimension, an estimate of I is given by:

$$\widetilde{I}(x,y,z) = \sum_{p=0}^{N} \sum_{q=0}^{p} \sum_{r=0}^{q} \lambda_{p-q,q-r,r} P_{p-q}(x)P_{q-r}(y)P_r(z) \quad (4)$$

The computation of the 3D Legendre moments can be performed using the fast method proposed by Hosny [12]. Translation and scale invariance are achieved by reformulating the Legendre moments in Eq. 2 by replacing (x, y, z) by $(\frac{x-x_0}{A}, \frac{y-y_0}{A}, \frac{z-z_0}{A})$ where (x_0, y_0, z_0) are the coordinates of the shape centroid and A is its volume.

3.2. Introducing a shape constraint into the multi-phase level-set framework

First, a set of training shapes are used to learn a fetus envelope shape model via Legendre moments. Then, the previously presented 3D multi-phase framework is updated accordingly to take into account the shape prior into the segmentation process.

Shape learning. As in [4], we used a L_2 distance to compare the evolving shape and the reference ones. Since we do not know which fetus positions and shapes are more likely to appear in the currently segmented image, all the N_s training reference shapes might be considered as equiprobable, which leads us to the following mixture of Gaussians:

$$P(L) = \frac{1}{N_s \sigma \sqrt{2\pi}} \sum_{k=1}^{N_s} \exp(-\frac{|L - L_k^{ref}|^2}{2\sigma^2}) \quad (5)$$

where N_s is the number of reference shapes, L the vector of Legendre moments $\{L_{pqr}\}$ of a considered shape and L_k^{ref} the vector of Legendre moments of the kth reference shape.

Given β the weight of the shape prior, the energy function can thus be re-written as:

$$E = E_{im} + \beta E_p(L) \quad (6)$$

with the shape prior term computed on the Legendre moments of the phase to constraint:

$$E_p(L) = -ln(P(L)) \qquad (7)$$

Iterative segmentation process. Since we want to control only the shape of the fetus envelope, we constrain only the phase containing it. The phase is chosen according to it statistics in order to match fetal pixels distribution. The other ones are evolved based only on gray-level statistical appearance models as explained in steps 2 to 5 of the following optimization procedure:

Do

1. Initialize $\{\phi_j\}_{j=1,2}$ as $\{\phi_j^0\}_{j=1,2}$

2. Evolution of $\{\phi_j\}_{j=1,2}$ by minimizing Eq. 1 using Euler-Lagrange equations according to gray-level homogeneity measures:

$$\{\phi_j^n\}_{j=1,2} \rightarrow \{\phi_j^{n+1}\}_{j=1,2} \qquad (8)$$

$$\{\phi_j^{n+1}\}_{j=1,2} \rightarrow \{\chi_i^{n+1}\}_{i=1,4} \qquad (9)$$

$$\{c_i^n\}_{i=1,4} \rightarrow \{c_i^{n+1}\}_{i=1,4} \qquad (10)$$

3. Computation of translation and scale invariant Legendre moments for one χ_i (here χ_1)

$$\chi_1^{n+1} \rightarrow L_{pqr} \qquad (11)$$

4. Update of L_{pqr} via gradient descent

$$L'_{pqr} = L_{pqr} - \beta \frac{\partial E_{prior}}{\partial L_{pqr}} \qquad (12)$$

5. Shape reconstruction from Legendre moments

$$L'_{pqr} \rightarrow \chi_1^{n+1} \qquad (13)$$

6. Phases update

$$\chi_1^{n+1} \rightarrow \{\phi_j^{n+1}\}_{j=1,2} \qquad (14)$$

$$\{c_i^{n+1}\}_{i=1,4} \rightarrow \{c_i^{n+1}\}_{i=1,4} \qquad (15)$$

Until no shape change occurs in two consecutive iterations

3.2.1. Parameterization

Time step. Since Legendre moments are sensitive to noise and the iterative estimates remain approximate, the shape reconstruction from moments tends to over-smooth the resulting shape. Since we are dealing with noisy images where precise boundaries are difficult to determine even for a human expert, the segmented phases need to evolve slowly to reach the correct tissue delineation. Too much smoothing can lead the segmentation process to miss the right partition into homogeneous tissues. Therefore, we decided to alternate between relaxation and enforcement of the shape prior, computing steps 2 to 5 only 1 upon k iterations (k was usually set to 2 in our experiments). The global time step Δt was set to 0.1 as in [7].

Choice of β. Since the time step has been relaxed and in order to guide efficiently the segmentation process toward the right shape, one has to choose a high weighting value. The β value was empirically set to 0.8 for all the performed experiments. This value leads to satisfactory results for all the tested data.

A comparison of the segmentation results obtained with the segmentation algorithm without and with the shape constraint is shown in Figures 2 (c) and (d). As seen on these figures, using the envelope prior improves the fetus body envelope segmentation but some maternal tissues remain attached to the fetus along the lower uterus boundaries. To adress this issue, a post-processing step is used as explained next.
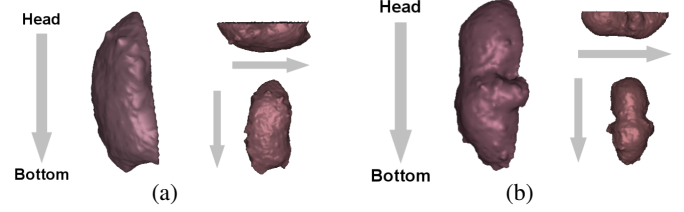

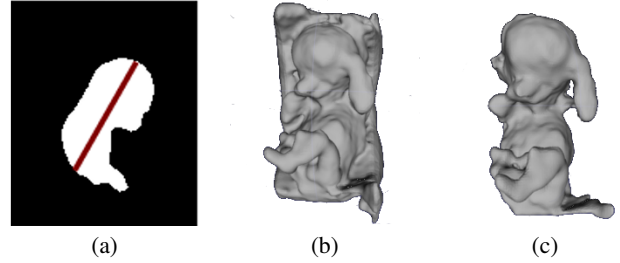**Fig. 3**. Back model of a (a) 10 WA old fetus. (b) 13 WA old fetus.

Fig. 4. (a) Crown-rump measurement. (b) 3D fetus reconstruction without post-processing. (c) Result after post-processing.

4. FETUS ENVELOPE SEGMENTATION

4.1. Algorithm

Since the approach deals with translation and scale invariant Legendre moments wich are not rotation invariant, the rotation parameters for the registration of the training set on the case being segmented have to be determined in an initialization step. Note that the parameters extracted during initialization are also used for post-processing.

Initialization The user is asked to select two landmarks corresponding to the ones used to compute the crown-rump measurement as shown in Figure 4 (a). The rotation between the fetus in the segmented image and the shape models is computed using the two given landmarks and the pre-positioned corresponding points on the template shapes. The scale factor can also be computed from the landmarks and could eliminate the need for scale invariance. These two landmarks also serve to compute the initialization of one of the two level-set functions using a cylindric shape with a diameter equal to the crown-rump measurement. The other initial level-set function is represented by a set of uniformaly distributed small cylinders over the rest of the image.

Post-Processing To take into account growth variations, a database composed of fetus back shapes was created based on a weekly-time scale, as illustrated in Figure 3. A back model for each week was derived by interpolating the shapes from this database for the missing weeks. Linear interpolation was performed along axes radiating from the middle of the crown-rump segment. For a given image to segment, the fetus age was then estimated from the crown-rump measurement and used to select the appropriate back model in the database. After rigidly registering it with the segmented fetus, the subset of the segmentation result located backward of both the back model and the coronal plane containing the crown-rump segment is removed according to the following operation: $I_{res} = (I_b \wedge I_{mask}) \vee I_f$, I_{mask} being the back model, I_b the image representing the back of the segmented fetus and I_f the image representing the front of the segmented fetus. Non-fetus tissues are efficiently removed by this processing, as illustrated in Figure 4.
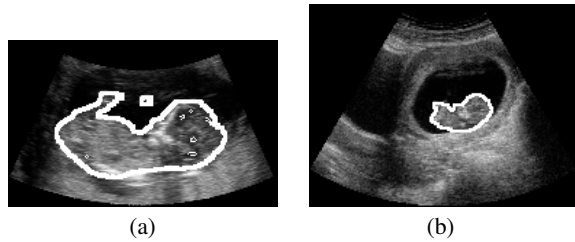
Fig. 5. Segmentation on 3D US cases at (a) 13 WA and (b) 10 WA.

Table 1. Quantitative results. Similarity, sensitivity and specificity indices computed between automatic and manual segmentations of the fetal envelope. The fetus age is given in weeks of amenorrhea (WA). *Legend: TP: True positive, TN: True Negative, FP: False positive, FN: False Negative*

fetus age (WA)	similarity index $\frac{\|Im_{res} \cap Im_{ref}\|}{\|Im_{res} \cup Im_{ref}\|}$	sensitivity $\frac{TP}{TP+FN}$	specificity $\frac{TN}{TN+FP}$
10	0.86	0.95	0.99
12	0.68	0.83	0.98
12	0.72	0.90	0.96
12	0.71	0.89	0.96
13	0.66	0.88	0.97
13	0.72	0.87	0.97
13	0.72	0.93	0.95
Mean Value	*0.72*	*0.89*	*0.97*

4.2. Results

The training data consisted of a set of 5 manually segmented 3D US cases (acquired using a 3D probe) representing fetuses at different ages (from 8 to 13 WA) and in different positions. Tests were carried out on a set of eleven 3D US cases for fetus aged from 8 to 13 WA which correspond to the first trimester of pregnancy where whole fetus body imaging is performed. For each case, a visual validation of the segmentation result was performed as illustrated in Figure 5. For seven of them a manual segmentation made by an expert was available and thus comparison between manual and automatic segmentations was carried out. Similarity, sensitivity and specificity indices were computed and are reported in Table 1. As shown in this table and in Figure 5, the proposed method provides accurate results with mean values of 0.72 for the similarity index, 0.89 for the sensitivity index and 0.97 for the specificity one. However, one can notice that in one case, presented in Figure 5 (a) (which corresponds to the one with a similarity index of 0.66 in Table 1), the segmented fetus tends to be smaller than the real one and sometimes some maternal tissues still remain attached to the fetus as in Figure 4 (c). This issue is a consequence of the error made during the registration of the back model with the output of the level-set segmentation procedure. Indeed, the back model used is a generic one and thus does not perfectly match the fetus one. Despite these errors, which remain limited, the segmentation process also gives satisfying results for all cases in terms of fetus shape preservation as seen in Figures 2 (f) and 5 (b).

5. DISCUSSION AND CONCLUSION

In order to segment the fetal envelope in 3D US images, a shape-guided multi-phase level-set segmentation framework has been presented in this paper. This 3D segmentation method embeds statistical priors on pixels distributions in the different parts of the utero-fetal unit and a shape prior on the fetus envelope. Shape information is encoded with Legendre moments and shape priors were learned over a variety of cases. Initialization of the segmentation process is performed semi-automatically by asking the user to determine

the crown-rump measurement. A post-processing step is also performed in order to clean the segmentation results from the remaining maternal tissues using a generic back model of a fetus. Tests on clinical cases provided satisfying results when compared visually and quantitatively to manual segmentations. Due to the small size of the dataset, the initial crown-rump measurement remains underexploited in the proposed method. Indeed, the stage of fetal growth based on this measurement is only used during the post-processing step to determine the most suitable back shape mask. However, with a larger training set, we could automatically detect the most suitable shapes of the training sets to be used. Indeed, using only fetal envelope shapes belonging to fetuses from the same gestational age would lead to a more accurate prior. Finally, the segmentation framework presented in this paper could be extended in a sequential way to segment also internal fetal structures (e.g. brain) on 3D US images.

6. REFERENCES

[1] J. A. Noble, "Image analysis of the human fetus and newborn - developing new clinical tools for perinatal care," in *ISBI*, 2012, pp. 490–492.

[2] L. Gupta, R. S. Sisodia, V Pallavi, C. Firtion, and G. Ramachandran, "Segmentation of 2D fetal ultrasound images by exploiting context information using conditional random fields," in *EMBC*, 2011, pp. 7219–22.

[3] J. Anquez, E. D. Angelini, G. Grangé, and I. Bloch, "Automatic segmentation of ante-natal 3D ultrasound images," *IEEE Transactions on Biomedical Engineering*, 2013, in press.

[4] A. Foulonneau, P. Charbonnier, and F. Heitz, "Multi-reference shape priors for active contours," *International Journal of Computer Vision*, vol. 81, no. 1, pp. 68–81, 2009.

[5] J. Wojak, E. D. Angelini, and I. Bloch, "Introducing shape constraint via Legendre moments in a variational framework for cardiac segmentation on non-contrast CT images.," in *VISAPP*, 2010, pp. 209–214.

[6] Y. Zhang, B. J. Matuszewski, A. Histace, and F. Precioso, "Statistical shape model of Legendre moments with active contour evolution for shape detection and segmentation," in *Computer Analysis of Images and Patterns*, vol. 6854, pp. 51–58. 2011.

[7] L. A. Vese and T. F. Chan, "A multiphase level set framework for image segmentation using the Mumford and Shah model," *International Journal of Computer Vision*, vol. 50, pp. 271–293, 2002.

[8] M. E. Leventon, W. E. L. Grimson, and O. Faugeras, "Statistical shape influence in geodesic active contours," in *CCVPR*, 2000, pp. 316–323.

[9] A. Tsai, A. Yezzi, W.M. Wells III, C.M. Tempany, D. Tucker, A. Fan, W.E.L. Grimson, and A. Willsky, "A shape-based approach to the segmentation of medical imagery using level sets," *IEEE Transactions on Medical Imaging*, vol. 22, no. 2, pp. 137–154, 2003.

[10] D. Cremers, "Dynamical statistical shape priors for level set based tracking," *IEEE Transactions on Pattern Analysis and Machine Intelligence*, vol. 28, no. 8, pp. 1262–1273, 2006.

[11] M. Rousson and N. Paragios, "Prior knowledge, level set representations & visual grouping," *International Journal of Computer Vision*, vol. 76, no. 3, pp. 231–243, 2008.

[12] K. M. Hosny, "Fast and low-complexity method for exact computation of 3D Legendre moments," *Pattern Recognition Letters*, vol. 32, no. 9, pp. 1305–1314, 2011.